**RiESTech**
*Recent in Engineering Science and Technology*

MBI

*Article*

# Measuring Thermal Conductivity and Magnetic Strength Using Low-Cost Sensors Based on an Open-Source Platform Arduino

**Nazhmi Fadhila [1], Filia Solagratia Takasumiang [1], Hanandira Wistikhirana [1], Yudha Dewangga [1], Rafi Pradaya Andareska [1], Agus Edy Pramono [2,*], Iman Setiyadi [2]**

[1] Study program of Applied Bachelor of Manufacturing Technology, Politeknik Negeri Jakarta, Indonesia
[2] Magister Program in Applied Manufacturing Technology Engineering, Politeknik Negeri Jakarta, Indonesia
* Correspondence: agus.edypramono@mesin.pnj.ac.id

**Abstract:** The use of low-cost sensors controlled by an open-source microcontroller (Arduino) is investigated in this study to measure electrical, thermal, and magnetic parameters, and to evaluate the feasibility of using these sensors for future extraction of intrinsic material properties such as thermal conductivity and magnetic response. The MAX6675 and HMC5883L sensors, together with an SS49E Hall sensor, were used to monitor a carbon rod supplied with 29.9 V DC. The MAX6675 thermocouple sensor recorded surface temperatures in the range of 48–50 °C, showing consistent trends when cross-checked against multimeter readings. The HMC5883L magnetic sensor measured an average magnetic field strength of approximately 8.65 G, remaining within stable control limits across all trials. Meanwhile, the electrical current recorded manually from the digital display of the power supply due to the absence of an installed current sensor averaged 0.21 A during testing. Minor signal interference was observed when multiple sensors operated simultaneously, indicating the need for electrical isolation or signal multiplexing in future designs. These findings demonstrate that low-cost open-source sensors can produce consistent and interpretable data for basic material characterization, supporting the development of affordable instrumentation as a practical alternative to commercial measurement systems. Accordingly, this work emphasizes sensor consistency and measurement feasibility rather than reporting final thermal conductivity values.

**Keywords:** Low-cost sensors; Arduino; Thermal conductivity; Magnetic strength

**Citation:** Fadhila, N., Takasumiang, F. S., Wistikhirana, H., Dewangga, Y., Andareska, R. P., Pramono, A. E., Setiyadi, I. (2026). Measuring Thermal Conductivity and Magnetic Strength Using Low-Cost Sensors Based on an Open-Source Platform Arduino. Recent in Engineering Science and Technology, 4(02), 59–72. Retrieved from https://www.mbi-journals.com/index.php/riestech/article/view/118.

Academic Editor: Vika Rizkia

Received: 16 June 2025
Accepted: 3 February 2026
Published: 30 April 2026

**Publisher's Note:** MBI stays neutral with regard to jurisdictional claims in published maps and institutional affiliations.



## 1. Introduction

Many researchers have been using low-cost sensors controlled by cheap microcontrollers as an economical alternative to expensive commercial tools over the years [1], [2], [3], [4], [5], [6]. A common microcontroller used is open-source platform Arduino that can be used for many purposes. Arduino project itself has many board models, one of which is Arduino UNO. Arduino UNO is a microcontroller board based on ATmega328P microcontroller. It has 14 digital pins, 6 analog pins, 5V and 3.3V rail, 3 ground pins, for I2C communications SDA and SCL pin and a USB connection to connect to a computer. Arduino IDE is used to write and upload code to the board.

Some low-cost sensors incorporate hall elements, such as Allegro™ ACS712 current sensor. ACS712 has a copper conduction path inside which current flows and generates magnetic field. Hall IC then converts the magnetic field into proportional voltage. There are 3 variants of ACS712 which have different current sensing ranges from 5A, 20A and 30A. ACS712 has been used as an economical choice for measuring AC or DC current. A study used ACS712 to measure current discharged by Battery Discharger Board (BDB), a device that allows discharging Li-ion cells with a programmable profile. While ACS712 is low-cost, the measurements are noisy. In order to filter the noise, Kalman Filter (KF) a linear quadratic estimation is used and the signal produced becomes smooth [7]. The high

noise recorded using ACS712 in some cases are thoroughly considered. An example is in this study that develops a test bench for checking the quality of electric vehicle chargers. A range of sensors are used and ACS712 is considered for AC and DC current measurements. However, the author noted that the hall-effect principle is not suitable for AC current measurement and used OP-AMP 358 in a non-inverting amplifier mode instead. Filter circuits are used for both AC and DC measurements. A DHT11 temperature sensor is also used to monitor internal components of the charger [8]. Current and other parameters produced by photovoltaic panels need to be monitored and, in this study, an ESP32 board and ACS712 30A are used with additional Bluetooth features. The study showed that the ACS712 experienced intense noise of 130 mA. To filter the noise, instead of using KF, an alternative simple method is proposed using 470nF capacitor. The result shows the system is able to monitor photovoltaic panels especially in isolated places where the internet network is absent [9]. An ESP32 board is also used in this study developing an IoT system to monitor batteries used in electric vehicles. ACS712 30A is used to measure current and LM35, a high voltage analog temperature sensor is also used. The study designed a voltage divider network consisting of 1kΩ and 2kΩ resistors to achieve a full scale reading of 30A within the 3.3V maximum limit of I/O pins and the ADC input. A Sallen-Key active low pass filter is used to achieve precise and accurate current measurements within short durations (below 10ms). A noticeable difference is observed after the filter is installed [10]. Voltage irregularities are often responsible for damaging electrical equipment. In order to protect the equipment, an experimental system was developed using Arduino UNO board, ZMPT101B for measuring voltage and ACS712 for measuring AC current. The system helps protect overvoltage and undervoltage conditions in a single-phase power supply [11]. This study used ACS712 5A sensor to monitor current consumed by Dynamixel MX 64 AT servo motor used in mobile robotic platforms. The system used Arduino Mega 2560 board and ADS1115, a 16-bit ADC, to improve the resolution and measure currents in the order of tens of milliamps. The experiment showed that the largest error for ACS712 compared to a multimeter is 13.75% and the lowest error at 0.38% [12]. This wide range of accuracy error trend would continue to this study of comparing the measurements from ACS712 controlled by ATMega328P to a high precision network power analyzer Chauvin Arnoux C.A 8335. The largest error observed is 19.38%. In home appliances including hot dryer, fluorescent lamp, heater and a laptop the largest accuracy error is 3.43% [13]. ACS712 is also used in the machining industry. A device using ACS712, and an Arduino board is developed to measure RMS current in drilling machines. The measurements are taken every 50ms and recorded with the help of LabView. The study explored ways to monitor drill bit condition and using current signature can effectively detect tool wear. ACS712 is able to detect current rising with respect to increased friction as drilling depth increases. Rate of current also rises high during initial wear of the drill bit. With more usage, the current amplitude increases thus indicating wear [14].

Another example of a low-cost sensor using hall elements is SS49E. SS49E are small devices that are commonly used to detect magnetic field. It has a wide magnetic range of ±1000G with a supply voltage of 5V. Unlike ACS712, the SS49E doesn't require filtering circuit due to the integrated circuitry that features low noise output and an additional amplifier to strengthen the signal. A demonstration of the capability of the SS49E is showed in this study of recording the magnetic field produced by underwater cable. Four SS49E sensors and a DS18B20 temperature sensor are used in this experiment. DS18B20 is used to account for temperature variations and thus make the magnetic field measurements more accurate. Arduino Nano board is chosen as the microcontroller and an additional feature of a microSD card module to record data. The difference between the theoretical magnetic field and the measured magnetic field is within range considered admissible. The results are that the underwater measurements are very accurate ±0.3% on average and both in and out of salt water. The study showed that the device could work

and store magnetic field measurements up to 150 m under the sea [15]. Other studies have shown that SS49E is a perfectly viable alternative to measure magnetic field strength in a wide range of applications. This study used SS49E and Arduino board to control the magnetic field of a MAGLEV system to be constant by adjusting current running through the coil. Magnetic field strength generated by a ferrosilicon core with 1250 turns and a current of 0.58A is measured by SS49E sensor to be 0.0811T or 811G and be able to levitate a body of 0.1 kg [16]. In thermodynamics field, SS49E also saw usage. The magnetic field affecting the performance of thermoelectric cooler is measured using SS49E and an Arduino Mega 2560 board. LM35 temperature sensor is also used. To simulate the magnetic field, a system is built consisting of two magnetic coils to produce 2T of magnetic intensity. The result of the study shown that coefficient of performance (COP) increases with the magnetic field. From 0.875T to 1.25T, the maximum enhancement of COP can be found at 1.25T [17]. In the food industry, SS49E and Arduino Nano board is used to measure EMF to evaluate its effects to the quality of the cocoa beans from the fermentative process. To generate the EMF, lab scale Helmholtz coils are used to generate variable density magnetic field of 1 to 120mT. The measurements are read using LabView. The result of the study revealed that magnetic field densities of 5 to 42mT improves yield and flavor of the cocoa beans and 80mT correlates to low yield and bitterness [18]. In another study, a 49E sensor which is similar to SS49E and a small neodymium magnet is integrated to a DIY filament extruder machine. Arduino Nano board is used to process the output from the sensor and control the extruder speed. The change of the filament diameter can be calculated by detecting the magnetic field strength. The experiment showed that the obtained tolerance of the filament diameter is ±0.1 mm. However, the produced filament is not up to the industry standards of tolerance up to ±0.05 mm for precision FDM printing [19]. An alternative to SS49E sensor is MLX-90215 sensor. In this study, the sensor is used with a 16-bit ADC USB-6210 to measure magnetic strength of iron oxide nanoparticles coated with either $SiO^2$ and $TiO^2$. The measurements are compared to the SQUID magnetometer model MPMS-XL. At the saturation region, the largest error is at 10% and the lowest at 0.4% [20]. A1302 sensor is also a popular alternative to SS49E. A study used A1302 and LMT86 temperature sensor with additional components such as a solar panel and a network system to monitor structural crack in a monumental architecture. The system could detect displacement and measure in tens of micrometers [21].

Another parameter, besides current and magnetic strength, commonly measured using low-cost sensor is temperature. There are various types of temperature sensors, from NTC thermistor, resistance temperature detectors (RTDs), thermocouples and semiconductors. One of which is easy to interface using Arduino boards are thermocouples using a MAX6675 that digitize signal from type-K thermocouple. This converter outputs the measurements in resolution up to 0.25°C and is able to read maximum temperatures of 1024°C. To interface with an Arduino board, SPI communication is used. There are several studies using MAX6675 and demonstrated its capabilities in lab and even in industrial scale. MAX6675 has a similarity with ACS712, with them being noisy. However, several studies have proven that either with or without an additional circuit to improve the accuracy of the sensors by filtering the noise or by adding Analog-to-Digital Converter (ADC) to improve resolution, the measured data is deemed accurate enough for it to be reliable. Four type-K thermocouples with MAX6675 each are used with Arduino Mega 2560 board and a microSD card module to measure temperatures of a water in a heater controlled using a voltage regulator in this study. Similar to ACS712, KF is used to improve the readings accuracy and reduce the noise [22]. This study discusses the application of a low-cost smart system for a heat treatment of AISI 1040 steel. To monitor the temperatures, a type-K thermocouple with MAX6675 is connected to an Arduino UNO board with an additional feature of wireless communications using NRF240L01 receiver and ESP8266 board. Using the smart system, the hardness of AISI 1040 is measured at 232 HV whilst from traditional normalizing heat

treatment process measured at 234 HV. The temperature error observed is ±3oC with no additional filtering process required [23]. This study explored the efficiency in energy of thermoelectric devices (TEDs) when operated as thermoelectric coolers (TECs). To measure temperature, the author used 3 MAX6675 connected to an ESP32 board to measure the hot side of the TEC. Due to MAX6675 not able to read below 0°C, to measure the cold side the author proposed MAX31855, which is similar to MAX6675, but deemed too difficult to use with the SPI interface and DS18B20 is used instead requiring only one digital pin and is also more affordable [24]. This study developed an IoT device to use with any commercial furnace lab or oven to measure temperatures using MAX6675. The system helps the user observe real-time temperature data and can detect fire or overheating. The average reading compared to commercial thermometer difference is observed at 0.34% which is accurate enough for this safety system [25]. This study uses MAX6675 and an Arduino board to control the heater temperature of a filament extruder. A simple bang-bang control is implemented to control the heater if it has reached the desired temperature to extrude the filament [26]. This study utilized MAX6675 to measure the temperature of the pot in a design of smart electric cooking stove. There are several problems regarding the temperature readings, including a lag in actual change of temperature and the study suggests that direct contact of the sensor to the heating surface is required and also coating the thermocouple with heat insulation material to avoid convectional heat to affect the thermocouple [27]. A unique implementation of MAX6675 is in this study used for temperature control of electrically floated samples with a thermocouple in direct contact with it. The device is electrically insulated from the CVD chamber and the Arduino UNO board is connected to a ZigBee Wi-Fi unit. The difference between thermocouple reading and an infrared pyrometer can be +25°C at 140-minute mark while the temperature reading of the MAX6675 stays constant at 650°C throughout the experiment. The study revealed that this error is due to a change in emissivity [28]. This study developed a system using MAX31855K to digitize signal from type-K thermocouple and Arduino to process it. The system is used to measure the temperature of a ladle transporting molten steel and the performance of the system is evaluated under harsh environments. The system shows great durability and did not fail while measuring up to 1250°C temperatures at prolonged periods of time and the accuracy of the data meets the industry quality standards [29]. A study developed a system that was developed for characterization of thermoelectric generators (TEGs) for energy harvesting using MAX31855 for temperature measurements and ACS712 5A sensor for current acquisition. It's shown that the temperature error reaches 12% while the current measurements have an error of 4%, both without calibration measures [30].

The aim of this study is to make a low-cost and easy to fabricate device, based on affordable sensors and an Arduino board to measure thermal conductivity and magnetic strength of a material. While low-cost sensors have been used to easily measure parameters in a range of applications, few have been used to process and calculate from the data to obtain material properties, especially in thermal conductivity [31].

Accordingly, this study aims to develop a low-cost and easy-to-fabricate Arduino-based instrumentation prototype (GTAM) and to evaluate its feasibility for future extraction of intrinsic material properties especially for thermal conductivity and magnetic response). In this work, feasibility is assessed by demonstrating synchronized monitoring of thermal, magnetic, and electrical parameters under controlled DC excitation and by examining measurement consistency during repeated trials.

This work contributes (i) an integrated multi-sensor prototype built from affordable modules, (ii) a practical acquisition workflow that includes real-time display and automatic CSV data logging to support repeatable experiments and post-processing, and (iii) a stability summarization approach using control-chart boundaries (CL, UCL, and LCL) to describe sensor consistency across trials. The observed interference and

placement sensitivity indicate that isolation/multiplexing and fixed sensor mounts are needed to improve future measurements.

## 2. Design, Material and Construction method

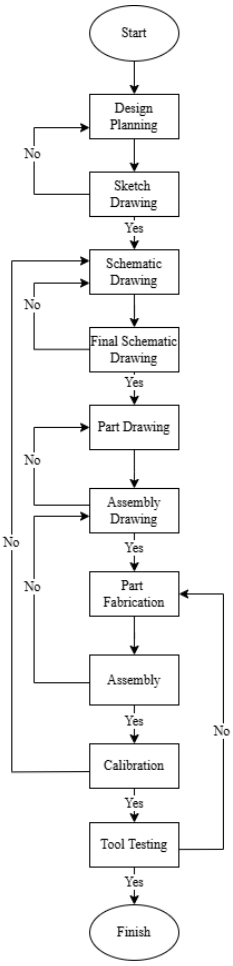


**Figure 1.** Stages of design and construction of the GTAM

In designing this measuring instrument, several software are used to help, such as Solidworks (SW) to help design, in addition because this measuring instrument is based on Arduino, Arduino IDE is used to help in the electrical field. Figure 1 explains more clearly about the flow of design and construction stages.

- Design planning, initial design planning that includes objectives, tool specifications, and system requirements, which will produce output in the form of an initial design planning document (design brief).
- Sketch drawing means making a rough sketch to express ideas and concepts for the physical form of the tool.
- Schematic drawing, creating a schematic diagram of the electrical system and sensors. The output produced is a wiring diagram shown in Figure 3.
- Part drawing, steps for making technical drawings of each component of a measuring instrument.
- Assembly drawing, a drawing that shows how all the components are assembled and produces output in the form of an exploded view as shown in figure 2.
- Part fabrication, the process of physically making each component based on the drawings that have been made.
- Assembly, assembling all mechanical and electronic parts into one unit.

- Calibration is required to set the initial value and system settings to comply with measurement standards.
- Tool testing, comprehensive testing of tool functionality to ensure all systems work as they should.

## 3. Results and Discussion

### 3.1. Visual Design and System Diagrams

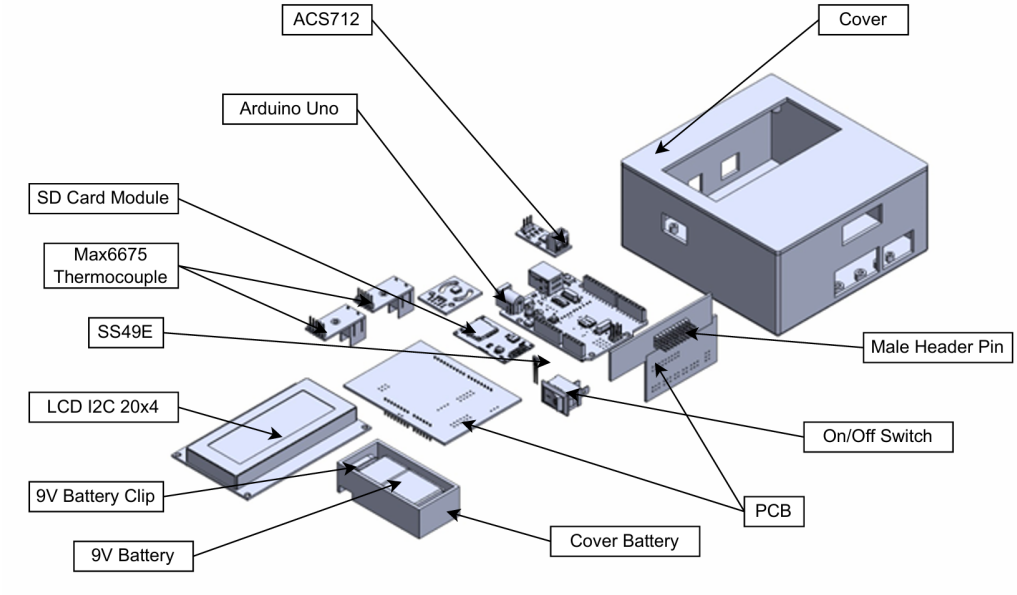


**Figure 2.** Exploded of GTAM

The design of the measurement device results in the exploded view configuration shown in Figure 2. In the exploded view, the dimensions of each component are intentionally omitted as a form of copyright protection by the designer. Several components in this design are commercially available modules, while others—such as the casing, PCB, and battery cover—are custom-fabricated parts developed to support the system's integration and portability.

This design article groups the components of the measurement device into several major categories:

a) Electronic Module Components
The electronic module components of the measurement device consist of several integrated modules that support the system's functionality. The Arduino Uno serves as the central microcontroller, responsible for acquiring data from various sensors and executing control operations. Temperature measurement is handled by the MAX6675 Thermocouple Module, which interfaces with the Arduino via the SPI communication protocol for accurate thermal readings. The ACS712 current sensor is used to measure the electric current in the circuit, while the SS49E magnetic sensor captures magnetic field intensity in analog form, allowing for precise detection of magnetic variations. To log data, the device uses an SD Card Module, which stores the collected sensor information for further analysis or archival. Real-time readings are presented through the LCD I2C 20x4 display, which uses the I2C communication interface to efficiently communicate with the Arduino, minimizing the use of digital pins and simplifying wiring.

b) Power Supply Components
The system is powered using a 9V battery connected via a 9V battery clip, with an on/off switch integrated on the PCB to control power flow to the Arduino and modules. This ensures ease of operation and portability without the need for external power adapters.

c) Mechanical & Structural Components

The mechanical and structural components of the device are designed to provide a stable foundation and protective enclosure for all electronic modules. The Printed Circuit Board (PCB) serves as the primary base, facilitating the physical arrangement and electrical interconnection of all sensors and modules. Male header pins are integrated onto the PCB to allow modular, plug-and-play connections, simplifying assembly and maintenance. The entire system is enclosed within a custom-designed cover, which not only protects the internal components from mechanical impact and environmental exposure but also features cutouts that ensure accessibility to the LCD display, power switch, and sensor interfaces. Additionally, a dedicated battery cover secures the 9V battery in place, ensuring both safety and ease of replacement. This structural integration enhances both the functionality and durability of the measurement device.

All components are arranged in a compact and modular layout to ensure easy maintenance, future upgrades, and reliable field operation. The enclosure ensures durability and ease of use in various environmental conditions.

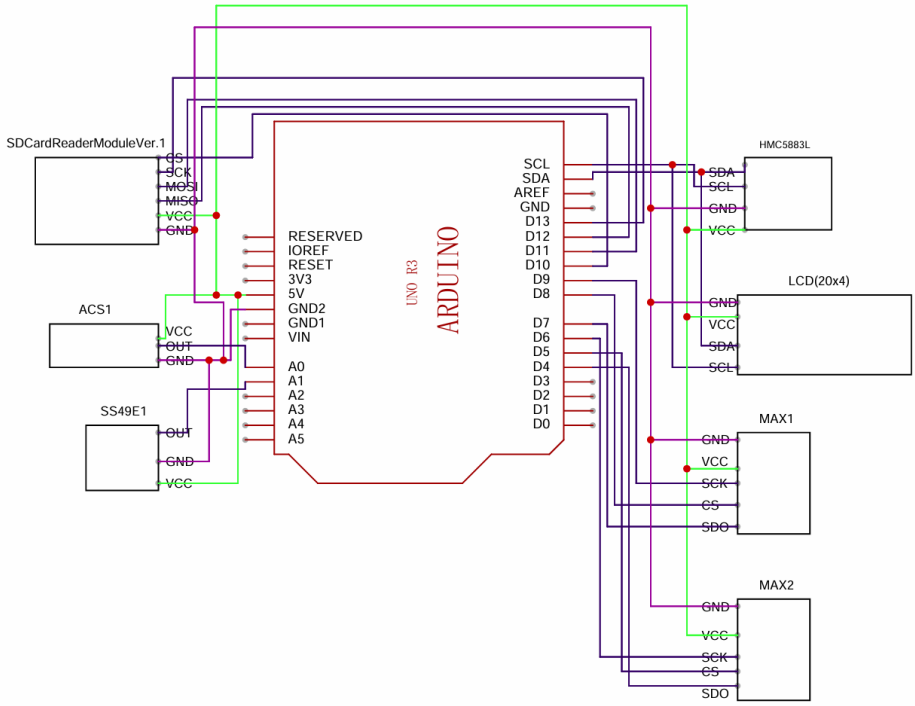


**Figure 3.** Wiring Diagram of GTAM

The Arduino Uno serves as the central controller, receiving a 5V power supply. The SD Card Reader Module is connected via SPI (pins D10–D13) to store data in CSV format. The LCD 20x4 uses I2C communication (SDA: A4, SCL: A5) to display real-time readings. The HMC5883L magnetic field sensor also uses I2C protocol (SDA: A4, SCL: A5). Two MAX6675 thermocouple modules are connected via SPI using separate CS pins (D2 and D3). Analog sensors, ACS712 (current sensor) and SS49E (hall-effect magnetic sensor), are connected to analog pins A0 and A1 respectively. This configuration allows synchronized acquisition and logging of temperature, magnetic field, and current data.

### 3.2. System Testing Result and Analyst

**Table 1.** Data of Experience

| Experiment | Ampere (A) | T1 (°C) | T2 (°C) | Gauss (G) | X (mT) | Y (mT) | Z (mT) |
|---|---|---|---|---|---|---|---|
| 1 | 0,21 | 48,75 | 37,25 | 8,45 | -18,09 | 4,9 | 17,6 |
| 2 | 0,22 | 49 | 37,25 | 8,55 | -18,09 | 4,9 | 17,53 |
| 3 | 0,2 | 49,5 | 37,5 | 8,73 | -17,91 | 4,8 | 17,44 |
| 4 | 0,2 | 49,5 | 37 | 8,64 | -18,55 | 5 | 17,55 |
| 5 | 0,21 | 49,75 | 37,75 | 8,91 | -18,18 | 5,1 | 17,44 |
| 6 | 0,22 | 49,75 | 37,75 | 8,82 | -18 | 5,31 | 17,53 |
| 7 | 0,22 | 49,25 | 37,5 | 8,64 | -17,82 | 5 | 17,6 |
| 8 | 0,21 | 49,75 | 37,25 | 8,36 | -17,91 | 5,1 | 17,48 |
| 9 | 0,2 | 49,75 | 37,25 | 8,45 | -18,09 | 4,9 | 17,44 |
| 10 | 0,21 | 50 | 37,25 | 8,36 | -18,09 | 5 | 17,58 |
| 11 | 0,22 | 50 | 37,25 | 8,55 | -17,91 | 5 | 17,58 |
| 12 | 0,21 | 50 | 37 | 8,82 | -18,36 | 5,1 | 17,51 |
| 13 | 0,2 | 49,75 | 37,25 | 8,73 | -18,18 | 4,9 | 17,48 |
| 14 | 0,22 | 49,5 | 37,25 | 8,91 | -18,45 | 5,2 | 17,48 |
| 15 | 0,21 | 50,25 | 37,25 | 8,82 | -18,55 | 5,2 | 17,46 |

The test was conducted by passing DC current through the carbon rod using a regulated power supply at 29,9V. The MAX6675 thermocouple sensor was mounted directly on the rod to measure the surface temperature, while the HMC5883L magnetic field sensor was positioned approximately 15 cm next to the rod. Each trial data of temperature, magnetic field, and current values were recorded simultaneously every 1 second.

Among all the sensors installed, only the thermocouple (MAX6675) produced stable and interpretable readings. The dual thermocouple setup experienced interference when both were installed simultaneously on the carbon rod, so it was decided to rely on only one sensor for valid data, in this experiment the thermocouple sensor relied on was the one shown in column T1.

It should be noted that the current readings in the table do not come from the system's internal sensors, but are taken manually from the current display on the power supply during testing.

Based on the collected test data, visualization is carried out in the form of graphs for each measurement parameter, namely electric current (amperes) shown in figure 4, temperature from the T1 sensor (MAX6675), gauss from HMC5883L sensor, and magnetic field components on the X, Y, and Z axes from SS49E sensor. The magnetic field components on the X, Y, and Z axes are expressed in millitesla (mT), which is a standard SI-derived unit used to represent magnetic flux density. Current data is recorded manually from the power supply display, while other data is obtained from automatic sensor readings.

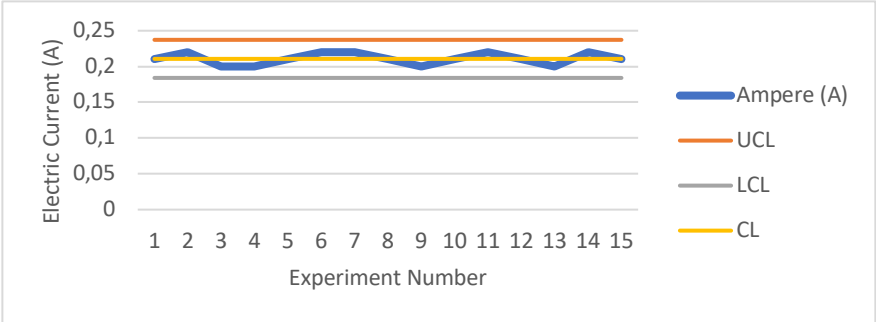


**Figure 4.** Graph of Ampere Measurement

The control chart shown in Figure 4, Figure 5, Figure 6 and Figure 7 use three reference lines, namely the Center Line (CL), Upper Control Limit (UCL), and Lower Control Limit (LCL), to evaluate the stability of the measurement results. The CL represents the average value of the observed data and reflects the normal operating condition of the system. The UCL and LCL define the upper and lower boundaries of acceptable data variation, respectively, which are statistically determined based on the dispersion of the measured values. Data points falling within these limits indicate that the system operates under stable and controlled conditions, while points exceeding the UCL or falling below the LCL suggest potential anomalies, disturbances, or measurement errors. In this experiment that shown in Figure 4, all current data remain within the control limits, indicating consistent and reliable system performance.

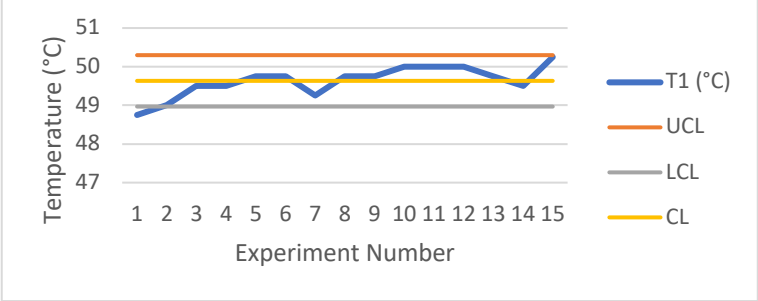


**Figure 5.** Graph of T1 Measurement

From the temperature graph of the T1 sensor shown in Figure 5, the measured temperature generally exhibits a stable and gradual increase over the experimental trials and remains within the defined control range. One data point, observed in the first trial, falls outside the control limits, indicating a deviation from both the Upper Control Limit (UCL) and Lower Control Limit (LCL). This deviation is attributed to the initial transient condition of the system, where the temperature had not yet reached a steady-state after power-up. Following the first trial, all subsequent temperature readings fall within the control limits, demonstrating stable system performance and reliable surface temperature measurement of the carbon rod under DC current excitation.

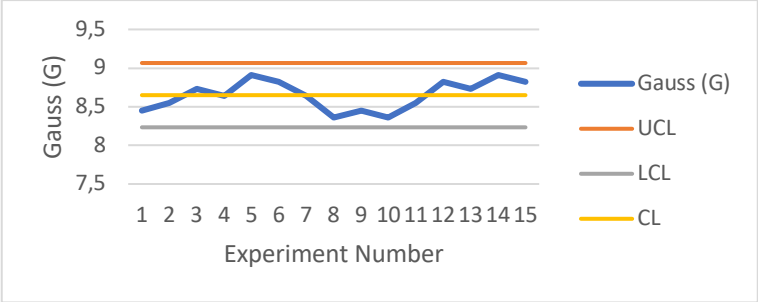


**Figure 6.** Graph of Gauss Measurement

Magnetic field measurements were carried out using the HMC5883L sensor placed at a distance of about 15 cm next to the carbon rod. The data obtained were in the form of magnetic field strength values (in Gauss units). The measurement results showed that all magnetic field strength values were within the control limits (UCL and LCL), with an average of 8.649 Gauss. As shown in Figure 6, no data was found that deviated from the control limits (CL), indicating that the sensor provided relatively stable and acceptable results for the purposes of observing the trend of magnetic field changes due to current flow in the carbon rod.

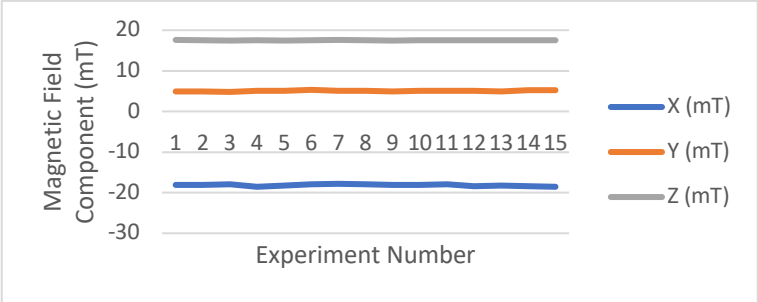


**Figure 7.** Graph of Magnetic Field Measurement

The measurement data of magnetic field components on the X, Y, and Z axes shown in figure 7 relatively small and stable fluctuations in value throughout 15 experiments. However, although the graph shows relative stability, it should be noted that the sensor position has not been permanently fixed. The sensor is only placed at a distance of about 15 cm next to the carbon rod without using a jig. Therefore, the use of a jig is highly recommended in further testing to improve the accuracy and repeatability of vector magnetic field component measurements.

Overall, this work goes beyond reporting raw sensor outputs by demonstrating a complete measurement workflow, including real-time monitoring, automatic CSV logging, and post-processed stability evaluation using control limits (CL/UCL/LCL). The consistent trends observed across trials indicate that this integrated workflow is practical for repeatable low-cost instrumentation prototyping.

### 3.3. Technical Issues and Solutions

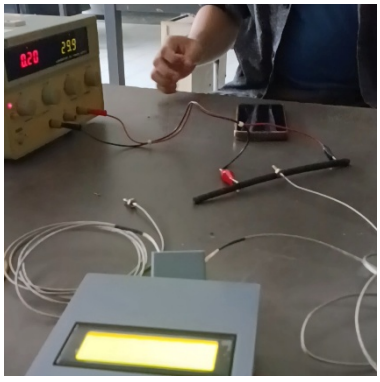

**Figure 8.** Documentation of Experiment

During the system assembly and testing process, several technical issues were found that affected the quality and consistency of the data. One of the main obstacles occurred in the use of two MAX6675 thermocouple sensors simultaneously attached directly to the carbon rod. The test results showed that one of the sensors could not provide a valid temperature reading or experienced interference (error). This is thought to be caused by signal interference due to the installation position being too close, as well as possible conflicts in data communication from the sensors. To overcome this, it was decided to use only one thermocouple sensor (T1) which was proven to provide the most stable and reliable results.

The next problem is related to reading the current value. In this system, there is no ACS712 current sensor installed due to device and time limitations. Instead, the current value is taken directly from the digital display on the power supply used to flow current to the carbon rod. Although this method is not an automatic reading through the system, the current value from the power supply is quite stable and is used as a reference in

recording data. The use of accurately calibrated current sensors is still recommended for future tool development.

Another problem was found in the installation position of the HMC5883L and SS49E magnetic field sensors. Both sensors were simply placed next to the carbon rod at a distance of about 15 cm without using a jig or fixed support. This unfixed position has the potential to cause small variations in orientation and distance between experiments, which can affect the results of the magnetic field readings, especially in the X, Y, and Z axes. Although the graph shows general data stability, the use of a jig is essential to ensure the accuracy and repeatability of the measurement results in further testing.

In addition, in the first experiment, the temperature reading by the T1 sensor showed a value that was outside the upper control limit (UCL). This is thought to have occurred because the system had not reached a stable thermal condition when data collection began. Therefore, it is recommended to provide a pre-heating period before data recording begins to ensure that all components are in a steady-state condition.

Overall, various technical problems found have been identified and analyzed. Temporary solutions have been implemented, and several recommendations for improvement have been prepared for the development of the tool to be more stable and accurate in the future.

### 3.4. Interpretation and Future Improvements

Based on the test results, this measuring instrument system shows quite good performance in recording temperature and magnetic field data simultaneously. The MAX6675 thermocouple temperature sensor provides the most stable results with a measurement range of 48–50°C, especially from the first sensor (T1) which is used as the main reference because readings from two sensors simultaneously cause errors in the measurement.

One of the advantages of this system is the automatic data storage feature. Each measurement result of temperature, magnetic field, and current is displayed in real-time on a 20x4 LCD, and simultaneously stored in CSV format on an SD card, making it easier for users to document and analyze data further.

However, there are still some technical limitations that need to be fixed:

- Current reading is not yet automatic, because internal current sensors such as the ACS712 are not installed on this device due to system limitations, so current data is still recorded manually from the power supply display.
- Calibration of the magnetic field unit has not been carried out, due to limited reference tools or calibration standards. As a result, the displayed gauss value is still relative and its accuracy in international units cannot be guaranteed.
- The absence of a jig to position the magnetic sensor causes possible inconsistencies in position between experiments.

As a future development, several things that are recommended include:

- Addition of an automatic current sensor so that all parameters can be recorded directly by the system.
- Making a jig or fixed mount for the HMC5883L and SS49E sensors to improve accuracy and repeatability.
- Calibration of the magnetic field sensor against a standard magnetic field source or using a verified reference tool.

With these improvements, the measuring instrument that has been developed can be upgraded towards a portable, automatic physical monitoring system that is ready to be used in the context of research, laboratory testing, or simple industrial needs.

## 4. Conclusions

This study developed and evaluated a low-cost, Arduino-based instrumentation prototype (GTAM) for synchronized monitoring of thermal, magnetic, and electrical parameters on a carbon rod under DC excitation. During system testing, temperature measurements obtained using the MAX6675 thermocouple (T1) were stable and interpretable, with surface temperatures recorded in the range of 48–50 °C, and only an initial transient point outside the control limits before the system reached steady-state behavior. Magnetic measurements using the HMC5883L sensor remained within the control limits across all trials, yielding an average magnetic field strength of 8.649 Gauss and demonstrating consistency for trend observation. The electrical current during testing averaged 0.21 A, but it was recorded manually from the power-supply display because the ACS712 current sensor was not installed in the device at the time of experimentation.

Several practical limitations were identified. The dual MAX6675 configuration showed interference when two thermocouple modules were mounted simultaneously on the rod therefore, a single thermocouple channel (T1) was used for valid temperature acquisition. In addition, magnetic sensor positioning was not fixed using a jig, which may introduce small variations between trials, and magnetic calibration could not be performed due to limited reference standards; thus, the magnetic readings should be interpreted primarily for repeatable trend monitoring rather than absolute calibration-grade measurement.

Overall, the results indicate that low-cost, open-source sensors integrated in a compact platform can produce consistent and interpretable data for basic characterization and instrumentation prototyping. Future improvements should prioritize (i) installing an automatic current sensor for fully integrated electrical monitoring, (ii) applying electrical isolation or signal multiplexing to reduce multi-sensor interference, (iii) implementing fixed-position fixtures (jigs) to improve measurement repeatability, and (iv) conducting sensor calibration against verified reference tools to strengthen quantitative interpretation for future material-property extraction.

**Acknowledgments:** The designer and author would like to express their gratitude to Mr. Iman Setiyadi who acted as a donor by providing funds for the design and manufacture of this gauss, temperature and ampere (GTAM) measuring instrument.

**Conflicts of Interest:** "The authors declare no conflict of interest."

## References

[1] V. A. Balogun, B. I. Oladapo, A. O. M. Adeoye, J. F. Kayode, and S. O. Afolabi, "Hysteresis analysis of Thornton (IP6, IP12E and TH5V) magnetic materials through the use of Arduino microcontroller," *Journal of Materials Research and Technology*, vol. 7, no. 4. pp. 443–449, 2018. doi: 10.1016/j.jmrt.2017.05.018.

[2] P. F. Pereira and N. M. M. Ramos, "Low-cost Arduino-based temperature, relative humidity and CO2 sensors - An assessment of their suitability for indoor built environments," *Journal of Building Engineering*, vol. 60. 2022. doi: 10.1016/j.jobe.2022.105151.

[3] A. S. Ali, Z. Zanzinger, D. Debose, and B. Stephens, "Open Source Building Science Sensors (OSBSS) A low-cost Arduino-based platform for long-term indoor environmental data," *Build. Environ.*, vol. 100, pp. 114–126, 2016, doi: https://doi.org/10.1016/j.buildenv.2016.02.010.

[4] D. A. McGranahan, "FeatherFlame: An Arduino-based thermocouple datalogging system to record wildland fire flame temperatures in agris," *Rangeland Ecology and Management*, vol. 76. pp. 43–47, 2021. doi: 10.1016/j.rama.2021.01.008.

[5] J. F. D. F. Araujo, E. B. M. Junior, and L. A. F. Mendoza, "A Simple Portable Magnetometer Based on Magnets and Hall-Effect Sensors Capable of Measuring Magnetic Properties," *Appl. Sci.*, vol. 12, no. 24, 2022, doi: 10.3390/app122412565.

[6] E. C. Prima, S. Karim, S. Utari, R. Ramdani, E. R. R. Putri, and S. M. Darmawati, "Heat Transfer Lab Kit using Temperature Sensor based ArduinoTM for Educational Purpose," in *Procedia Engineering*, 2017, pp. 536–540. doi: 10.1016/j.proeng.2017.03.085.

[7] P. L. dos Santos, T. P. A. Perdicoúlis, P. A. Salgado, and J. C. Azevedo, "Kalman filter for noise reduction of Li-Ion cell discharge current," *IFAC-PapersOnLine*, vol. 56, no. 2. pp. 9582–9587, 2023. doi: 10.1016/j.ifacol.2023.10.261.

[8] J. Jency Joseph, F. T. Josh, S. Leander Gilbert, and S. Leander Gilbert, "A test bench on quality checking for electric vehicle chargers," in *Materials Today: Proceedings*, 2021, pp. 8176–8181. doi: 10.1016/j.matpr.2021.02.554.

[9] Z. Didi and I. El Azami, "Experimental Analysis and Monitoring of Photovoltaic Panel Parameters," *Int. J. Adv. Comput. Sci. Appl.*, vol. 14, no. 2, pp. 151–157, 2023, doi: 10.14569/IJACSA.2023.0140219.

[10] S. Haldar, S. Gol, A. Mondal, and R. Banerjee, "IoT-enabled advanced monitoring system for tubular batteries: Enhancing efficiency and reliability," *e-Prime - Adv. Electr. Eng. Electron. Energy*, vol. 9, 2024, doi: 10.1016/j.prime.2024.100709.

[11] D. D. Tung and N. M. Khoa, "An Arduino-Based System for Monitoring and Protecting Overvoltage and Undervoltage," *Eng. Technol. Appl. Sci. Res.*, vol. 9, no. 3, pp. 4255–4260, 2019, doi: 10.48084/etasr.2832.

[12] G. Constantin *et al.*, "Monitoring the Current Provided by a Hall Sensor Integrated in a Drive Wheel Module of a Mobile Robot," *Machines*, vol. 11, no. 3, 2023, doi: 10.3390/machines11030385.

[13] Đ. Lazarević, M. Živković, Đ. Kocić, and J. Ćirić, "The utilizing Hall effect-based current sensor ACS712 for true RMS current measurement in power electronic systems," *Sci. Tech. Rev.*, vol. 72, no. 1, pp. 27–32, 2022, doi: 10.5937/str2201027L.

[14] J. Gokulachandran and B. Bharath Krishna Reddy, "A study on the usage of current signature for tool condition monitoring of drill bit," in *Materials Today: Proceedings*, 2019, pp. 4532–4536. doi: 10.1016/j.matpr.2020.09.696.

[15] V. Luna, R. Silva, E. Mendoza, and I. Canales-García, "Recording the Magnetic Field Produced by an Undersea Energy Generating Device: A Low-Cost Alternative," *J. Mar. Sci. Eng.*, vol. 11, no. 7, 2023, doi: 10.3390/jmse11071423.

[16] A. H. Takinami, R. B. Cruz, B. L. S. de Lima, and F. Jesus de Almeida, "Design, simulation and development of a magnetic levitation system (MAGLEV)," *Results Phys.*, vol. 17, 2020, doi: 10.1016/j.rinp.2020.103115.

[17] M. S. Nassar, A. A. Hegazi, and M. G. Mousa, "Combined effect of pulsating flow and magnetic field on thermoelectric cooler performance," *Case Stud. Therm. Eng.*, vol. 13, 2019, doi: 10.1016/j.csite.2019.100403.

[18] T. M. Guzmán-Armenteros, L. A. Ramos-Guerrero, L. S. Guerra, S. Weckx, and J. Ruales, "Optimization of cacao beans fermentation by native species and electromagnetic fields," *Heliyon*, vol. 9, no. 4, 2023, doi: 10.1016/j.heliyon.2023.e15065.

[19] Z. T. Piotr *et al.*, "Hall effect diameter sensor integration in DIY filament extruder," in *Procedia Computer Science*, 2022, pp. 1437–1445. doi: 10.1016/j.procs.2022.09.200.

[20] J. F. D. F. Araujo, M. C. Costa, S. R. W. Louro, and A. C. Bruno, "A portable Hall magnetometer probe for characterization of magnetic iron oxide nanoparticles," *J. Magn. Magn. Mater.*, vol. 426, pp. 159–162, 2017, doi: 10.1016/j.jmmm.2016.11.083.

[21] T. Addabbo *et al.*, "A low cost distributed measurement system based on Hall effect sensors for structural crack monitoring in monumental architecture," *Meas. J. Int. Meas. Confed.*, vol. 116, pp. 652–657, 2018, doi: 10.1016/j.measurement.2017.11.050.

[22] R. Septiana, I. Roihan, and R. A. Koestoer, "Denoising MAX6675 reading using Kalman filter and factorial design," *Int. J. Electr. Comput. Eng.*, vol. 11, no. 5, pp. 3818–3827, 2021, doi: 10.11591/ijece.v11i5.pp3818-3827.

[23] D. Saber, H. M. Almalki, and K. Abd El-Aziz, "Design and building of an automated heat-treatment system for industrial applications," *Alexandria Eng. J.*, vol. 59, no. 6, pp. 5007–5017, 2020, doi: 10.1016/j.aej.2020.09.023.

[24] N. P. Bayendang, V. Balyan, and M. T. Kahn, "The question of thermoelectric devices (TEDs) in/efficiency—a practical examination considering thermoelectric coolers (TECs)," *Results Eng.*, vol. 21, p. 101827, Mar. 2024, doi: 10.1016/j.rineng.2024.101827.

[25] M. Hassan, A. Bhattacharjee, M. S. Azam, S. Aziz, M. A. Ali Shaikh, and M. S. Islam, "A smart device of data acquisition with emergency safety features for laboratory furnaces," *Results Eng.*, vol. 19, 2023, doi: 10.1016/j.rineng.2023.101357.

[26] S. Nithya Priya, S. Naveen Kumar, S. Prem Kumar, and K. K. Pradeep, "Design and fabrication of filament extruder with spooler," in *Materials Today: Proceedings*, 2021, pp. 221–223. doi: 10.1016/j.matpr.2021.03.103.

[27] C. Svosve and L. Gudukeya, "Design of A Smart Electric Cooking Stove," in *Procedia Manufacturing*, 2020, pp. 135–142. doi: 10.1016/j.promfg.2020.02.127.

[28] T. Shimada, T. Miura, W. Xie, T. Yanase, and T. Nagahama, "A thermocouple-based remote temperature controller of an electrically-floated sample for plasma CVD of nanocarbons with bias voltage," *Meas. J. Int. Meas. Confed.*, vol. 102, pp. 244–248, 2017, doi: 10.1016/j.measurement.2017.02.012.

[29] V. Chang and C. Martin, "An industrial IoT sensor system for high-temperature measurement," *Comput. Electr. Eng.*, vol. 95, 2021, doi: 10.1016/j.compeleceng.2021.107439.

[30] C. L. Izidoro, O. H. Ando Junior, J. P. Carmo, and L. Schaeffer, "Characterization of thermoelectric generator for energy harvesting," *Measurement*, vol. 106, pp. 283–290, Aug. 2017, doi: 10.1016/j.measurement.2016.01.010.

[31] A. Abed Gatea Al-Shammary, A. Caballero-Calvo, H. A. Jebur, M. Ismael Khalbas, and J. Fernández-Gálvez, "A novel heat-pulse probe for measuring soil thermal conductivity: Field test under different tillage practices," *Comput. Electron. Agric.*, vol. 202, 2022, doi: 10.1016/j.compag.2022.107414.